Macromolecules

Article

pubs.acs.org/Macromolecules

Enhancement of CO_2 Affinity in a Polymer of Intrinsic Microporosity by Amine Modification

Christopher R. Mason,[†,§] Louise Maynard-Atem,[†,∥] Kane W. J. Heard,[†] Bekir Satilmis,[†] Peter M. Budd,*[,†] Karel Friess,[⊥] Marek Lanč,[⊥] Paola Bernardo,[‡] Gabriele Clarizia,[‡] and Johannes C. Jansen*[,‡]

[†]School of Chemistry, University of Manchester, Manchester, M13 9PL, U.K.

[⊥]Department of Physical Chemistry, Institute of Chemical Technology, Technická 5, Prague 6, 166 28, Czech Republic

[‡]Institute on Membrane Technology (ITM-CNR), Via P. Bucci, cubo 17/C, 87036 Rende (CS), Italy

ABSTRACT: Nitrile groups in the polymer of intrinsic microporosity PIM-1 were reduced to primary amines using borane complexes. In adsorption experiments, the novel amine–PIM-1 showed higher CO_2 uptake and higher CO_2/N_2 sorption selectivity than the parent polymer, with very evident dual-mode sorption behavior. In gas permeation with six light gases, the individual contributions of solubility and diffusion to the overall permeability was determined via time-lag analysis. The high CO_2 affinity drastically restricts diffusion at low pressures and lowers CO_2 permeability compared to the parent PIM-1. Furthermore, the size-sieving properties of the polymer are increased, which can be attributed to a higher stiffness of the system arising from hydrogen bonding of the amine groups. Thus, for the H_2/CO_2 gas pair, whereas PIM-1 favors CO_2, amine–PIM-1 shows permselectivity toward H_2, breaking the Robeson 2008 upper bound.

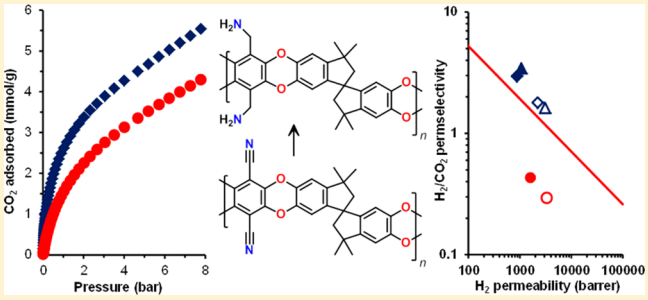

INTRODUCTION

Highly selective sorbents and membranes are desired for energy-efficient carbon dioxide capture and other gas separations. Polymeric molecular sieves, such as polymers of intrinsic microporosity (PIMs), offer advantages over inorganic and metal–organic porous materials in terms of processability. PIMs are glassy polymers that exhibit the characteristics of a microporous material (pore size <2 nm, as defined by IUPAC)[1] because their relatively inflexible, contorted backbones cannot pack space efficiently.[2] The archetypal membrane-forming PIM, referred to as PIM-1 (Scheme 1), is comprised of fused ring sequences interrupted by spiro centers and is prepared by a double aromatic nucleophilic substitution reaction between 5,5′,6,6′-tetrahydroxy-3,3,3′,3′-tetramethyl-1,1′-spirobisindane and tetrafluoroterephthalonitrile.[2] PIM-1 is soluble in common volatile solvents such as chloroform and tetrahydrofuran, and can be processed from solution into membranes that exhibit high permeability coupled with selectivity at the 2008 upper bound of performance for gas pairs such as CO_2/N_2. In recent years, there has been intensive effort aimed at achieving even higher performance, either through the synthesis of novel polymers such as Tröger's base PIMs,[3] or through chemical postmodification of PIM-1. The conversion has been reported of the nitrile groups in PIM-1 to carboxylic acid,[4,5] tetrazole,[6] thioamide,[7] and amidoxime[8] functionality. The amidoxime formation was described as "noninvasive functionalization" on the grounds that it improved carbon dioxide uptake without an adverse effect on physicochemical properties, although neither sorption selectivity nor membrane transport properties have been reported insofar as we are aware.

Scheme 1. Post-Modification of PIM-1 To Give Amine–PIM-1[a]

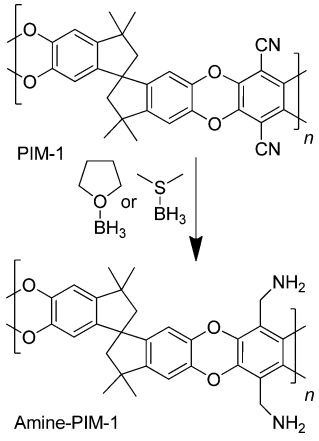

[a]PIM-1 in solution in THF was reduced using borane–THF complex under reflux. PIM-1 powders and membranes were reduced without dissolution using borane–dimethyl sulfide complex in diethyl ether, which swells the polymer to make the reactive sites accessible.

Received: September 9, 2013
Revised: January 10, 2014
Published: January 24, 2014

   dx.doi.org/10.1021/ma401869p | *Macromolecules* 2014, 47, 1021–1029

Amine modification of sorbents is frequently employed to introduce CO_2-philic functionality. In principle, the nitrile groups in PIM-1 could be reduced to primary amines using a variety of reagents. However, reactions that work well with low molar mass compounds are not always effective when applied to high molar mass polymers. Initial attempts to carry out the nitrile reduction with lithium aluminum hydride were unsuccessful. Borane complexes have been reported to be effective in reducing nitriles to primary amines with good yield.[9] Here we show that borane complexes can be used successfully to form amine−PIM-1 (Scheme 1). The incorporation of primary amines enhances CO_2 affinity, compared to the parent polymer, as demonstrated by gas adsorption experiments on powder and membrane samples, and by gas permeation studies of membrane samples. For the membrane samples, the reduction was carried out on preformed PIM-1 membranes, since the isolated amine−PIM-1 proved insoluble in common laboratory solvents and could not be cast from solution to form free-standing membranes. Reductions were similarly carried out on PIM-1 powders and on PIM-1 films coated onto glass slides.

EXPERIMENTAL SECTION

Materials. All solvents and reagents were used as purchased without further purification, unless stated otherwise. Methanol, ethanol (>99.5%), chloroform (≥99.5%, amylene stabilized), tetrahydrofuran (anhydrous), borane−tetrahydrofuran complex solution (1.0 M in THF, with <0.005 M sodium borohydride stabilizer) and borane−dimethyl sulfide complex solution (5.0 M in diethyl ether) were purchased from Sigma-Aldrich. PIM-1 was prepared as described previously.[2]

PIM-1 Membrane Preparation. PIM-1 (397 mg) was dissolved in $CHCl_3$ (19.6 mL) and stirred overnight. The membrane was then cast into a 10 cm Petri dish and the solution was allowed to evaporate over a period of 96 h. The membrane was exposed to a mixed ethanol: water (1:1) solution, which helped ease the film away from the edges of the dish. The membrane was allowed to dry in air over a period of 24 h, prior to conversion to the amine form.

Amine−PIM-1 Synthesis Using Borane−THF Complex. PIM-1 powder (1 g) was stirred in anhydrous tetrahydrofuran (THF) (65 mL) under an inert atmosphere. Upon dissolution, the mixture was cooled to 0 °C and 1.0 M borane−THF complex (12.24 mL, 12.24 mmol) was added dropwise to the reaction mixture. The reaction was set to reflux overnight with constant stirring, during which time the product precipitated. After cooling, ethanol (40 mL) was added dropwise to remove excess borane. The solid was collected and stirred overnight in 1.0 M methanolic HCl (60 mL), then separated by vacuum filtration and stirred in 5% aqueous NaOH solution (100 mL) for 3 h. The solid was washed repeatedly with water until neutral and dried at 120 °C under vacuum overnight. Yield: 846 mg (83%).

Amine−PIM-1 Synthesis Using Borane−Dimethyl Sulfide Complex. Since the amine−PIM-1 proved insoluble in common solvents and could not be cast from solution to form a membrane, further syntheses were carried out with borane−dimethyl sulfide complex in diethyl ether, a nonsolvent for the PIM-1 precursor. This enabled both membrane and powder samples of amine−PIM-1 to be prepared. Reduction was carried out using a 5.0 M borane−dimethyl sulfide complex in diethyl ether (19 mL, 95 mmol), with reaction conditions and washing procedures as above.

Amine−PIM-1 Films on Glass Slides. For contact angle measurements, thin films were prepared on glass microscope slides. PIM-1 (0.1206 g) was dissolved in $CHCl_3$ (15 mL) and stirred overnight. Glass slides were oven-dried and their surface covered with PIM-1 solution using a pipet, then quickly placed under a beaker in a fume cupboard and solvent allowed to evaporate for 4 h, before being oven-dried. The PIM-1-coated glass slides were placed in an oven-dried flange reactor under a nitrogen atmosphere and covered with 5.0 M borane−dimethyl sulfide complex in diethyl ether. The reaction vessel was immediately heated to reflux at 45 °C and slides removed at intervals over an 81 min period. The removed slides were placed in Petri dishes of ethanol and, when no longer liberating gas, were covered and left overnight, then transferred to Petri dishes of 1.0 M methanolic HCl, covered, and left overnight to soak. Subsequently, slides were transferred into 3% methanolic NaOH then, after a short time soaking (~5 min), into methanol. The methanol was neutralized (as tested with litmus paper) with a small amount of 3% methanolic NaOH, and the slides allowed to soak overnight. When early samples began to curl on drying, membranes were sandwiched between two glass slides in solution and compressed with a Petri dish while drying. The membranes were oven-dried for 3 h before the two slides were then separated and further oven-dried overnight.

Characterization Methods. Infrared (IR) spectra were recorded on a Bio-Rad FTS 6000 spectrometer equipped with an attenuated total reflectance (ATR) setup, and annexed to a Whatman FTIR purge gas generator. The spectra were recorded in the ATR mode, with a resolution of 0.25 cm^{-1}, a sensitivity of 1, and 16 scans in the range 4000−600 cm^{-1}.

Contact Angles were measured using a Krüss DSA 100 drop shape analyzer with deionized water. The drop needle diameter used was 0.52 mm and the machine dosing was set to S5 (M). The associated drop shape analysis program was used for computational analysis, with the drop type set to sessile and the drop subtype set to normal. The baseline for the contact angle measurements was manually detected.

High powered decoupling (Hpdec) magic angle spinning (MAS) solid state NMR spectra were collected using a Bruker Avance III 400 MHz instrument using an adamantane reference. A spinning rate of ~10 000 Hz was used with powder samples packed into a 4 mm zirconium rotor. Spectra were typically compiled from 6000 scans using a repetition time of 10 s and a spectral width of 600 ppm. Peak assignments were made with reference to Du et al.,[10] supported by ChemBioDraw (Cambridgesoft) predictions.

Thermogravimetric analysis (TGA) was performed under nitrogen, using a Mettler Toledo TGA/DSC Star system with a heating rate of 10 °C min^{-1} over a temperature range of 30−1000 °C.

Elemental analysis was carried out by the School of Chemistry Microanalysis Service, University of Manchester.

Gas Sorption. CO_2 and N_2 adsorption isotherms at a temperature of 0 °C (273.15 K) were obtained using a Micromeritics ASAP 2050 analyzer. Before sorption analysis, the sample was outgassed on the outgas port under vacuum at a temperature of 120 °C for a period of 16 h. Samples then underwent a further manual outgas on the analysis port under high vacuum at 120 °C for a period of 2 h. The measurement is based on determination of the total gas volume absorbed by the material. Helium was used for the freespace determination, both at ambient temperature and at 0 °C, after sorption analysis and additional manual outgas for 2 h.

Gravimetric adsorption/desorption experiments were performed using a homemade apparatus equipped with a calibrated McBain quartz spiral balance (spiral sensitivity 15.253 mg/mm). Experiments were performed at 25 ± 0.1 °C and at absolute pressures ranging from 0 to 17 bar. The detailed experimental procedure and buoyancy testing were described previously.[11] The sample was appended on the quartz spring by a tiny kanthal wire holder. The glass measuring chamber was evacuated before each measurement to a pressure lower than 10^{-3} mbar by a rotary oil pump (Trivac D4B, Oerlikon Leybold). A Leybold oil-mist filter eliminated (with 99.99% efficiency) contamination of the measuring chamber with oil vapors from the pump. After the exposure of the sample to a particular gas at a known pressure, the elongation of the quartz spiral due to gas sorption by the polymer membrane was monitored by a charge-coupled device (CCD, Sony) until the equilibrium state was reached. The average error of the mass determination reached approximately 30 μg.

Sorption data can be fitted with the well know dual-mode sorption model, describing the gas equilibrium concentration as a function of pressure:[12]

$$c = k_D p + \frac{C_H b p}{1 + b p} \quad (1)$$

dx.doi.org/10.1021/ma401869p | Macromolecules 2014, 47, 1021−1029

where c is gas concentration, p is gas pressure, k_D is the Henry's law constant, C_H is the Langmuir (monolayer) sorption capacity constant, and b is the Langmuir affinity constant. The gas concentration in the membrane at a given feed pressure is calculated from the gas solubility, S, in the membrane and the gas pressure, p:

$$c = S \times p \tag{2}$$

If indirect solubility data from permeation measurements are used (see below), then the mean pressure in the membrane must be considered for the calculation of the average permeant concentration:

$$p = p_{mean} = (p_{feed} + p_{permeate})/2 \tag{3}$$

When applied to permeation data, the above method is only exact if permeability coefficient P, diffusion coefficient D and solubility coefficient S are pressure independent, and thus it strictly applies in the case of linear rather than dual-mode sorption. In the case of pressure (or concentration) dependent transport, only complex models that must be solved numerically will give a more robust and correct quantitative description.[13,14]

Gas Permeation. Single gas permeation measurements were carried out at 25 °C and at a feed pressure of 1 bar in a fixed volume pressure increase apparatus (GKSS, Germany) in the time-lag mode.[13,15] The rotary vacuum pump was equipped with an alumina trap to avoid oil contamination of the membrane. The instrument is equipped with PC controlled pneumatic valves to allow response times of less than 0.5 s.[7] The gases were tested in the following order: He, H_2, N_2, O_2, CH_4, and CO_2. Before each experiment the membrane sample was carefully evacuated (10^{-2} mbar) to remove any dissolved gas species. Circular samples with an effective membrane area of 2.14 cm^2 were used. The thickness of the films was determined using a digital micrometer (Mitutoyo, Model IP65). The films were tested as received and after soaking in alcohol overnight and then drying in air at room temperature.

Permeability coefficient, P, and diffusion coefficient, D, were determined as described previously.[7] The gas permeability is expressed in barrer (1 barrer $=10^{-10}$ cm^3 cm cm^{-2} s^{-1} $cmHg^{-1}$ $= 3.35 \times 10^{-16}$ mol m m^{-2} s^{-1} Pa^{-1}). The solubility coefficient, S, for the gas in the polymer matrix was evaluated indirectly, assuming the validity of the solution-diffusion permeation model:

$$S = P/D \tag{4}$$

The ideal selectivity for a pair of gases, A and B, was calculated as the ratio of the individual single gas permeabilities. It can be decoupled into solubility-selectivity and diffusivity-selectivity:

$$\alpha_{A/B} = \frac{P_A}{P_B} = \frac{S_A}{S_B}\frac{D_A}{D_B} \tag{5}$$

RESULTS AND DISCUSSION

Amine Modification. Conversion of nitrile to amine was monitored by infrared spectroscopy (Figure 1), which showed loss of the nitrile stretch at 2239 cm^{-1} and the appearance of peaks at 3360 and 800 cm^{-1} which may be attributed to N−H stretch and N−H wag, respectively. The presence of nitrogen in the products was confirmed by elemental analysis (*e.g.*, for batch AM1-6: Calcd for $C_{29}H_{28}N_2O_4$: C, 74.33; H, 6.03; N, 5.98. Found: C, 71.67; H, 6.01; N, 5.13). Solid-state ^{13}C NMR spectra and assignments for PIM-1 and amine−PIM-1 powder prepared using borane−THF complex and borane−dimethyl sulfide complex are shown in Figure 2. On modification, there was a shift in the aromatic peak labeled 11, from 94 ppm in PIM-1 to 118 ppm in amine−PIM-1, and the appearance of a peak at 34 ppm, which may be assigned to the $-CH_2NH_2$ carbon. In PIM-1, the CN signal is hidden under the peak for carbons 6 and 9. Both complexes give degrees of conversion >90%, as estimated from IR and NMR data.

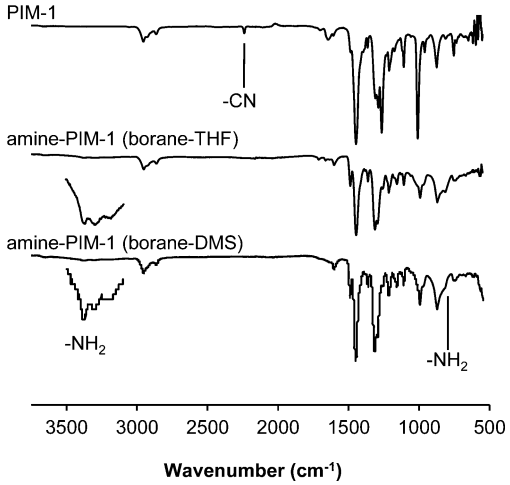

Figure 1. ATR-IR spectra of PIM-1(top) and amine−PIM-1 powder prepared using borane−THF complex (middle) and borane−dimethyl sulfide complex (bottom) with (inset) a magnification of the range 3100−3500 cm^{-1} for amine−PIM-1.

Amine modification increased the hydrophilicity of the polymer surface, as evidenced by a decrease in water contact angle from 86° to 66° for thin films on a glass substrate (Figure 3). Amine−PIM-1 membranes were found to be insoluble in chloroform, dichloromethane, hexane, tetrahydrofuran, dimethyl sulfoxide (DMSO), ethyl acetate, acetone, diethyl ether, dimethylacetamide, dimethylformamide, methanol, ethanol, 1-propanol, 2-propanol, 1-butanol, *n*-dodecane, toluene, mesitylene, 1,2-dichlorobenzene, 1,2,4-trichlorobenzene, m-cresol, pyridine, diethylamine, triethylamine, *N*′,*N*′-tetramethylethylenediamine, 1-methyl-2-pyrrolidinone, aqueous HCl and aqueous NaOH. They were also insoluble in solvent mixtures such as aqueous HCl/DMSO and aqueous NaOH/DMSO at temperatures up to 60 °C.

Thermogravimetric analysis of amine−PIM-1 showed *ca.* 7% weight loss in the temperature range 350−450 °C, prior to the degradation associated with the PIM-1 backbone (Figure 4). This is consistent with loss of NH_3, although it could also reflect a loss of residual solvent.

Chemical modification of PIM-1, especially with groups that are capable of hydrogen-bonding, frequently results in a reduction in the BET surface area determined from N_2 adsorption at −196 °C (77 K),[5−7] and in the case of amine−PIM-1, the low temperature N_2 adsorption was so slow that an isotherm could not be obtained. Indeed, gas permeation measurements (below) confirm that amine−PIM-1 is more size-sieving than PIM-1, and at lower temperature this will penalize especially the transport of the bulkier N_2 molecules. However, despite this loss of microporosity toward a nitrogen probe at −196 °C, high CO_2 uptake was achieved at 0 and 25 °C, as shown below. A similar loss of BET surface area coupled with enhanced CO_2 affinity was observed for tetrazole-modified PIM-1.[6]

Gas Sorption. Gas sorption results were obtained both at 0 °C, using a volumetric method, and at 25 °C, using a gravimetric method. Isotherms at 0 °C for amine−PIM-1 showed notably higher CO_2 uptake than the parent polymer (Figure 5a) and enhanced CO_2/N_2 sorption selectivity (Figure 5b). For a membrane sample, the ideal CO_2/N_2 sorption selectivity at 1 bar was 22 for amine−PIM-1, compared to 16 for the unmodified polymer. Sorption selectivity is especially

dx.doi.org/10.1021/ma401869p | *Macromolecules* 2014, 47, 1021−1029

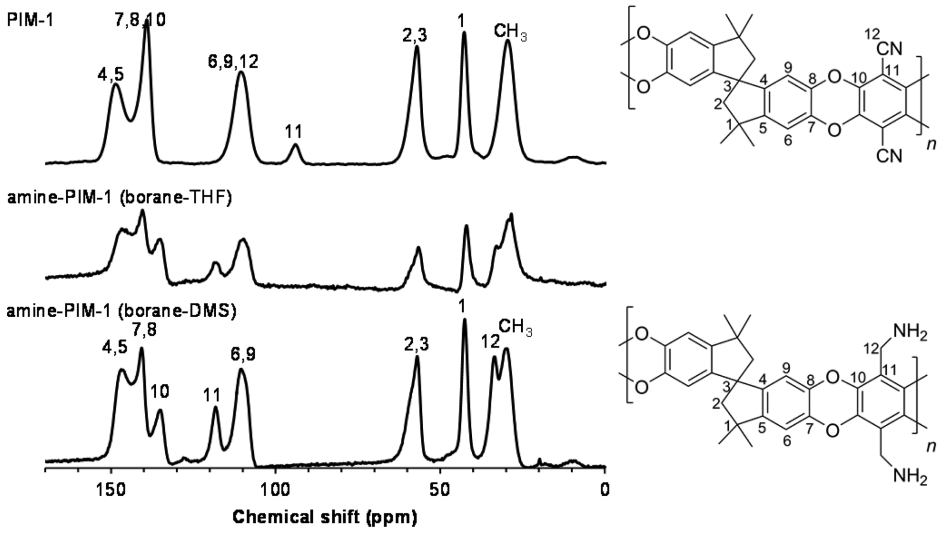

Figure 2. ^{13}C solid-state NMR spectra of PIM-1 (top) and amine–PIM-1 powder prepared using borane–THF complex (middle) and borane–dimethyl sulfide complex (bottom), showing peak assignments.

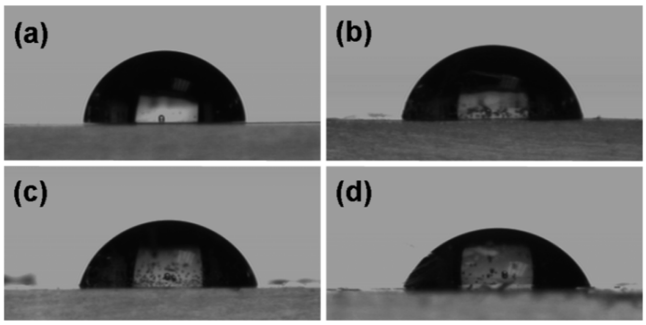

Figure 3. Drops of deionized water on film on glass slide of (a) unreacted PIM-1 (contact angle 86.3 ± 0.5°), and after (b) 21 min (contact angle 81.4 ± 0.6°), (c) 51 min (contact angle 77.0 ± 0.2°), and (d) 81 min (contact angle 66.2 ± 0.9°) reduction reaction.

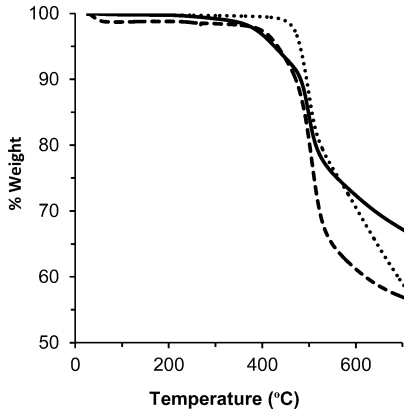

Figure 4. Thermogravimetric analysis of PIM-1 powder (short dashes), amine–PIM-1 powder prepared using borane–dimethyl sulfide complex (long dashes) and amine–PIM-1 membrane (solid line).

high at low pressure, confirming the much stronger interaction of CO_2 with the polymer as compared to N_2, as also suggested by the extremely steep start of the CO_2 sorption isotherm. From sorption measurements alone one cannot distinguish whether the steep curve is due to strong adsorption of CO_2 in very small pores (ultramicropores, <0.7 nm),[16] inaccessible to the slightly larger N_2 molecule, or to strong absorption by specific interaction or chemical reaction of the first monolayer of absorbed CO_2 in pores of any size.

A repeat adsorption run at 0 °C showed a lower CO_2 uptake (Figure 5c). The level of CO_2 uptake could be recovered, and even exceeded at high pressure, by repeating the purification procedure used after synthesis (soaking in methanolic HCl, then aqueous NaOH, washing with water and drying). It might be argued that the loss of capacity after the initial run is a consequence of specific binding of CO_2, perhaps through formation of carbamic acid or carbamate species, as has been observed for other amine-modified nanoporous materials.[17] However, the gravimetric CO_2 adsorption/desorption isotherm up to 17 bar at 25 °C (Figure 5d), while showing a slight hysteresis in the desorption curve, gives a virtually perfect return to the origin (only 0.3% weight change), confirming that there are no changes in the sample due to, for instance, irreversible chemical reaction. An alternative explanation of loss of capacity is rapid physical aging of the polymer in the presence of CO_2 at high pressure, as is discussed further in the context of permeation studies below.

Gravimetric sorption data at 25 °C (Figures 5d and 6) compare well with the volumetric data, giving slightly lower uptakes due to the higher temperature. Amine–PIM-1 clearly shows much higher CO_2/N_2 and CO_2/CH_4 sorption selectivity than the parent PIM-1. This is due to a significantly higher CO_2 sorption (60–20%) and a slightly lower methane and nitrogen sorption (0–15% and 5–40%, respectively).

Gas permeation. Table 1 lists gas permeabilities, and Table 2 ideal selectivities, for amine–PIM-1 membranes with various histories: (i) as cast, (ii) ethanol-treated, (iii) aged 18 months under ambient conditions and (iv) methanol-treated after aging. Reported values for another modification, thioamide–PIM-1,[7] are also given for comparison. The gas permeabilities of amine–PIM-1 are slightly lower than reported values for the parent polymer PIM-1,[18,19] and significantly higher than for thioamide–PIM-1. Whereas in PIM-1 and thioamide–PIM-1 the most permeable gas is CO_2, for amine–PIM-1 the H_2 permeability is higher than that of CO_2, evidencing a distinct size-sieving ability of the polymer, as has also been observed for the more rigid PIM-EA-TB.[3] While in the latter the increased

dx.doi.org/10.1021/ma401869p | Macromolecules 2014, 47, 1021–1029

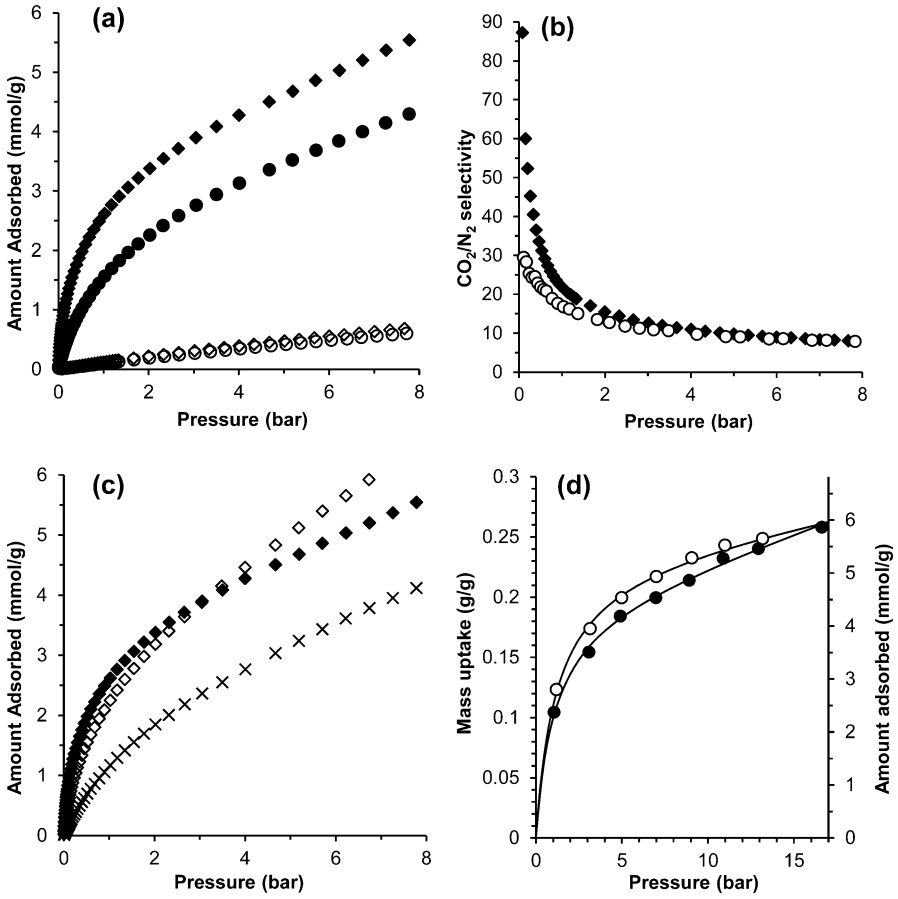

Figure 5. (a) CO_2 (filled symbols) and N_2 (open symbols) adsorption isotherms at 0 °C for PIM-1 (○, ●) and amine−PIM-1 (◊, ♦) membranes. (b) CO_2/N_2 ideal sorption selectivity at 0 °C for PIM-1 (○) and amine−PIM-1 (♦) membranes. (c) CO_2 adsorption isotherms at 0 °C for amine−PIM-1 membrane: First run (♦), repeat run (×) and after repurification (◊). (d) CO_2 adsorption (●) and desorption (○) isotherms from gravimetric sorption balance at 25 °C, with dual-mode fit, showing uptake in units of g/g (left axis) and mmol/g (right axis).

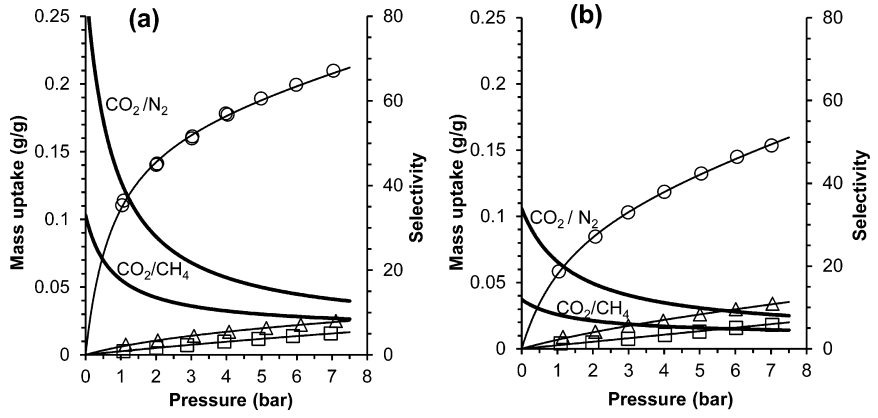

Figure 6. Gravimetric sorption isotherms (left axis) for CO_2 (○), CH_4 (Δ), and N_2 (□) in (a) methanol-treated amine−PIM-1 membrane (77 μm thickness) and (b) PIM-1 membrane (50 μm thickness). Thin solid lines represent the fit of the data according to the dual mode sorption model and thick solid lines (right axis) represent the corresponding ideal sorption selectivity calculated from the curve fit.

size-sieving ability derives from the higher rigidity of the EA-TB backbone, in amine−PIM-1 inter- and intrachain hydrogen bond formation between amine groups may be assumed to impart additional stiffness to the system.

Diffusion coefficients calculated from experimental time-lags, and solubility coefficients calculated using eq 4, are given in Table 3 for amine−PIM-1 and thioamide−PIM-1. It is noteworthy that for amine−PIM-1 the values of D for CO_2 are lower than those for N_2. In polymers the slightly smaller CO_2 molecule[20] is generally expected to diffuse faster than N_2, although many examples of the opposite situation exist.[21] This is consistent with strong immobilizing adsorption of CO_2, as demonstrated by Paul and Kemp,[22] who showed that the incorporation of a strongly adsorbing filler (zeolite 5A) into a polymer (silicone rubber) resulted in much greater time-lags (and hence lower apparent values of D) for CO_2 than for N_2. In the present case, very high affinity of amine−PIM-1 for CO_2 is qualitatively visible in Figure 6 as more pronounced dual mode

dx.doi.org/10.1021/ma401869p | Macromolecules 2014, 47, 1021−1029

Table 1. Gas Permeability Coefficients (P, barrer) for Amine−PIM-1 (This Work) and Thioamide−PIM-1 (Ref 7) Membranes with Different Histories at 25 °C

polymer	membrane state	He	H_2	O_2	N_2	CO_2	CH_4
amine−PIM-1	as cast	391	876	216	55.7	295	82.8
	ethanol-treated	863	2210	662	181	1230	259
	aged 18 months	483	1060	232	55	309	69
	methanol-treated	1200	3070	895	230	1890	303
thioamide−PIM-1	as cast	55	92	19	3.9	150	8.7
	ethanol-treated	270	610	140	37	1120	56

Table 2. Ideal Selectivity ($\alpha_{ij} = P_i/P_j$) for Various Gas Pairs in Amine−PIM-1 (This Work) and Thioamide−PIM-1 (Ref 7) Membranes with Different Histories at 25 °C

polymer	membrane state	He/N_2	H_2/CH_4	O_2/N_2	CO_2/N_2	CO_2/CH_4
amine−PIM-1	as cast	7.02	10.6	3.87	5.30	3.57
	ethanol-treated	4.77	8.54	3.66	6.81	4.76
	aged 18 months	8.81	15.4	4.31	5.65	4.48
	methanol-treated	5.22	10.1	3.90	8.24	6.24
thioamide−PIM-1	as cast	14.1	10.6	4.9	38.5	17.4
	ethanol-treated	7.3	10.6	3.8	30.3	19.6

Table 3. Gas Diffusion Coefficients (D, 10^{-8} cm^2 s^{-1}) and Solubility Coefficients (S, cm^3 [STP] cm^{-3} bar^{-1}) in Amine−PIM-1 (This Work) and Thioamide−PIM-1 (Ref 7) Membranes with Different Histories at 25 °C

	polymer	membrane state	He	H_2	O_2	N_2	CO_2	CH_4
D	amine−PIM-1	as cast	2290	1300	48.9	14.0	7.55	4.63
		ethanol-treated	5130	2780	141	40.0	25.3	12.9
		aged 18 months	2890	1790	62.6	15.8	7.0	4.52
		methanol-treated	5170	3970	223	59.8	39.3	17.9
	thioamide−PIM-1	as cast	1615	590	22	7.8	9.3	3.0
		ethanol-treated	1800	1250	49	15	21	4.4
S	amine−PIM-1	as cast	0.13	0.51	3.31	2.99	29.4	13.4
		ethanol-treated	0.13	0.60	3.51	3.39	36.5	15.1
		aged 18 months	0.125	0.445	2.83	2.60	33.0	11.4
		methanol-treated	0.174	0.579	3.02	2.88	36.1	12.7
	thioamide−PIM-1	as cast	0.03	0.12	0.66	0.37	12	2.2
		ethanol-treated	0.11	0.37	2.2	1.9	39	9.8

sorption behavior and high total sorption of CO_2. Quantitatively, the affinity is best expressed by the dual mode affinity factor, b, and the infinite dilution solubility, S_0:

$$S_0 = \lim_{p \to 0} \frac{dc}{dp} = k_D + C_H b \tag{6}$$

The latter represents the initial slope of the sorption isotherm, which is higher for amine−PIM-1 than for PIM-1 by a factor of nearly three, whereas it is equal for the inert gases methane and nitrogen (Table 4).

Table 4. Dual Mode Sorption Parameters and Infinite Dilution Solubility Obtained from a Least Squares Fit of the Sorption Isotherms of the Amine−PIM-1 and PIM-1 Samples in Figure 6

	gas	k_D, cm^3 cm^{-3} bar^{-1}	C_H, cm^3 cm^{-3}	b, bar^{-1}	S_0, cm^3 cm^{-3} bar^{-1}
amine−PIM-1	CO_2	3.14	82.2	1.31	110.5
	CH_4	1.61	30.3	0.251	9.22
	N_2	0.443	39.5	0.038	1.96
PIM-1	CO_2	3.92	52.8	0.715	41.7
	CH_4	3.58	30.2	0.200	9.62
	N_2	1.52	13.1	0.032	1.93

The perhaps surprising inversion of the diffusion coefficients of CO_2 and N_2 by strong affinity between CO_2 and the amine groups in the polymer backbone was recently also found for a novel PIM with Tröger's base units in the backbone,[3] showing unexpectedly low CO_2/N_2 selectivity and CO_2/CH_4 selectivity. This principle was previously demonstrated for amine-functionalized polysulfone[23] and has been reviewed by Lin and Freeman.[24] The net effect of increased polymer−penetrant interaction is a delicate balance between increased sorption, favoring transport, and possible "immobilization", penalizing transport. The result will vary from case to case but will always be negative if interaction is too strong.

For amine−PIM-1, treatment with ethanol increases from two to three times the permeability of most gases, and over four times that of CO_2, compared to the as cast membrane (Table 1). After 18 months the permeabilities and the selectivities return to values which are slightly higher than those of the as cast film. The decrease in permeability on aging is more significant for larger gases (O_2, N_2, CH_4, CO_2) than for smaller gases (He and H_2). The He/N_2, H_2/CH_4 and O_2/N_2 ideal selectivities, slightly reduced by ethanol soaking, increase upon aging. Glassy polymers typically present a permeability decline over time owing to relaxation of the macromolecular chains, a reduction of the total free volume and a rearrangement of the free volume element size and distribution, and consequent

dx.doi.org/10.1021/ma401869p | Macromolecules 2014, 47, 1021−1029

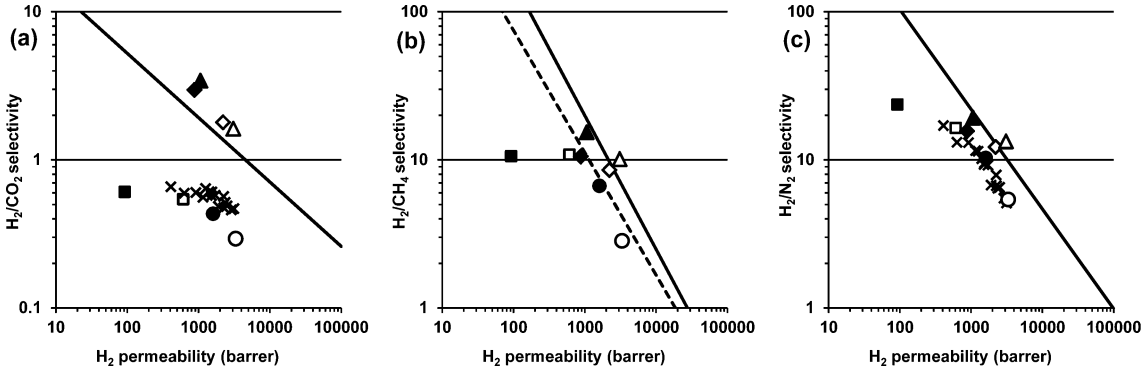

Figure 7. Double logarithmic "Robeson" plots of (a) H_2/CO_2, (b) H_2/CH_4 and (c) H_2/N_2 selectivity versus H_2 permeability showing Robeson's 2008 upper bound[29] (solid line), and for H_2/CH_4 the 1991 upper bound[30] (dashed line), with data for amine−PIM-1 as cast (♦), ethanol-treated (◊), after aging for 18 months (▲) and methanol-treated after aging (Δ), compared with literature data[19] for PIM-1 as cast (●) and methanol-treated (○), for thioamide−PIM-1[7] as cast (■) and ethanol-treated (□), and for PIM-1 hydrolyzed under various conditions[4] (×).

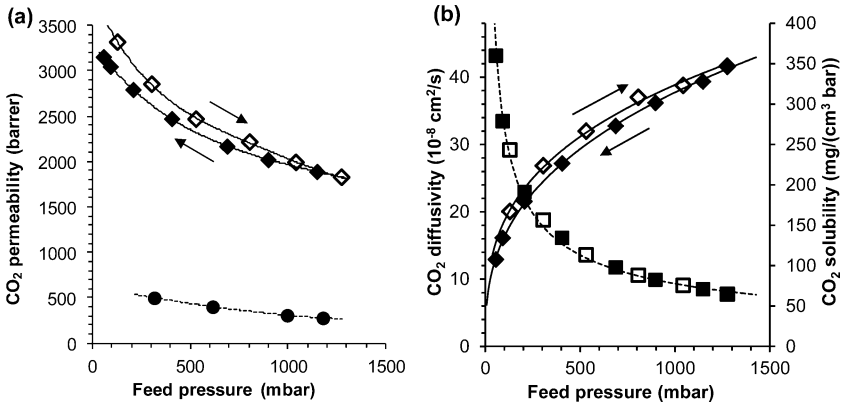

Figure 8. (a) CO_2 permeability (♦, ◊) and (b) CO_2 diffusion coefficient (♦, ◊) and CO_2 solubility coefficient (■, □) as functions of feed pressure for methanol-treated amine−PIM-1 (lines indicated as a guide to the eye). Open symbols are for results obtained on increasing pressure and closed symbols are for results obtained on decreasing pressure. Permeability of the as-cast membrane (●) is given for comparison.

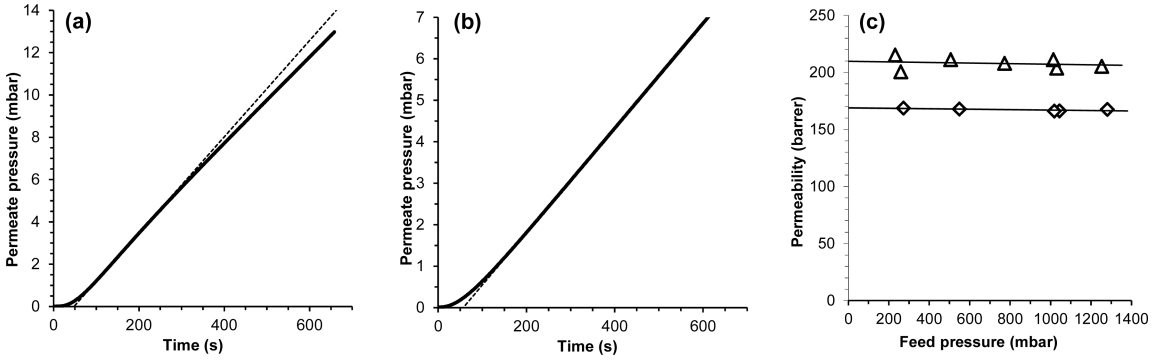

Figure 9. (a) Anomalous downward curvature in the time-lag curve of CO_2 (feed pressure 0.2 bar) and (b) normal curve shape in the time-lag curve of CH_4 (feed pressure 1.0 bar), for freshly methanol-treated membrane at 25 °C. Qualitatively, the same behavior is observed for as-cast and aged samples, and for measurements at different pressures. (c) Pressure dependence of the methane permeability (△) and nitrogen permeability (◊) of methanol-treated amine−PIM-1 membrane.

increase in polymer density.[25−27] This can be particularly evident in rigid and highly permeable polymers. Soaking in a lower alcohol reverses the effects of physical aging, as well as removing residues of casting solvent from the films,[19,28] and allows for a fair comparison of different superglassy polymers by eliminating the casting history. The permeability of the aged sample could thus be fully restored, and even increased, by soaking it in methanol (Table 1). The permeability of CO_2 increases over six times with respect to the as cast film. This confirms the higher effectiveness of methanol compared to ethanol, as observed in PIM-1.[19] The diffusion coefficient is more affected than the solubility by these conditioning procedures (Table 3), giving rise to an increased permeability, along with a slightly reduced selectivity for most gas pairs.

The high H_2 permeability of amine−PIM-1, coupled with good gas selectivities, locates amine−PIM-1 at or above the 2008 Robeson upper bounds[29] for some H_2 separations of technological relevance, such as H_2/CO_2, H_2/CH_4 and H_2/N_2

dx.doi.org/10.1021/ma401869p | Macromolecules 2014, 47, 1021−1029

(Figure 7), a particularly pronounced effect being observed for H_2/CO_2. For commercial application, higher selectivities would be required, but this work demonstrates the principle that changing a single functional group can lead to a complete reversal of properties.

As discussed above, the incorporation of basic nitrogen functionality enhances the CO_2 capture capacity. Nevertheless, based on pure gas permeation, amine−PIM-1 does not perform better toward CO_2 than PIM-1, and its performance for the CO_2/N_2 and CO_2/CH_4 gas pairs falls below the 2008 upper bounds.[29] The stronger interaction with the polymer matrix reduces the CO_2 diffusion rate, outweighing the relative increase in solubility, giving a net reduction of permeability as compared to other gases and to PIM-1. However, it is not unlikely that this behavior is reverted in mixed gases, where the strong CO_2 sorption is expected to depress permeability of larger molecules, for instance CH_4 in the case of biogas separations. This will be the subject of further studies.

In glassy polymers, gases with a high solubility in the polymer matrix typically show distinct dual-mode sorption behavior, resulting in a pressure dependent permeability. Thus, CO_2 permeation at different pressures revealed a decrease in the gas permeability as the feed pressure increases (Figure 8a), mainly due to a drastic reduction of the CO_2 solubility, whereas the diffusion coefficient increases moderately (Figure 8b). At the lowest pressures, the pressure dependence of the solubility (and permeability) is so high that significant changes occur in the permeate pressure range during a measurement run, manifesting itself as an unusual bend in the permeation curve of CO_2 (Figure 9a). In the same pressure range, nitrogen and methane behave normally (Figure 9b) and have a virtually pressure-independent permeability (Figure 9c), diffusivity, and solubility, and their permeation curves do not show any unusual curvature. Qualitatively, the same kind of behavior was observed in as cast and freshly methanol-soaked membranes.

Swelling, plasticization and/or aging phenomena may further enhance unusual transport behavior in polymer glasses. Figure 8a shows hysteresis in the CO_2 permeation due to notable aging of the freshly methanol-treated membrane during the approximately 10 h of the total measurement cycle. Aging is a well-known phenomenon in PIMs[31] and various approaches have been used to reduce this by chemical modification/cross-linking[32,33] or by use of mixed matrix materials.[34] The hysteresis is also observed in the diffusion coefficient (Figure 8b), which decreases with time, whereas the solubility is virtually unaffected and independent of time.

Interestingly, it was found that even the indirectly obtained CO_2 solubility data could be fitted fairly well with the dual-mode sorption model (Figure 10). However, there is a discrepancy when this is compared to the directly obtained sorption data. The difference between transport parameters from sorption and permeation is systematic and has recently been reviewed by Robeson et al.[20] In the present case, with very pronounced dual-mode behavior, the discrepancy becomes so strong that in spite of the apparently good qualitative description, the indirect solubility data cannot be used for quantitative analysis.

CONCLUSIONS

Borane complexes can be used successfully to reduce the nitrile groups in PIM-1 to primary amines, forming amine−PIM-1. Gas adsorption demonstrates that the incorporation of primary amines enhances the affinity for CO_2 and the CO_2/N_2 and CO_2/CH_4 sorption selectivity, introducing very distinct dual-mode sorption behavior for CO_2 even at low pressures. The affinity is so strong that, in membrane permeation experiments, CO_2 diffusion, and hence permeability, is reduced, but high permeabilities are obtained for small noninteracting gases (H_2 and He). Consequently, for the H_2/CO_2 gas pair, amine modification changes the polymer from being permselective toward CO_2 in PIM-1, to being permselective toward H_2 in amine−PIM-1, breaking the Robeson 2008 upper bound.

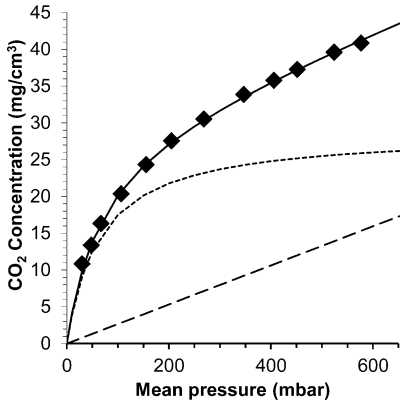

Figure 10. CO_2 sorption data (♦) obtained indirectly from permeability and diffusion coefficients with fit to the dual-mode sorption model (solid line) and the individual contributions of Langmuir sorption (short dashes) and Henry sorption (long dashes).

The high CO_2 sorption in amine−PIM-1 offers promising perspectives for further improvement in mixed gas permeation, where competitive sorption is expected to favor permeation of CO_2 over other species, and at higher pressures, where swelling and dilation is expected to give a further general increase of permeability. This will be the subject of further studies.

AUTHOR INFORMATION

Corresponding Authors

*(P.M.B.) E-mail: Peter.Budd@manchester.ac.uk. Telephone +44(0)161-275-4711.

*(J.C.J.) E-mail: jc.jansen@itm.cnr.it. Telephone +39 0984 492031.

Present Addresses

§(C.R.M.) Hexcel Composites Ltd., Duxford, Cambridge, CB22 4QD, U.K.

∥(L.M.-A.) Department of Health, Quarry House, Leeds, LS2 7UE, U.K.

Author Contributions

The manuscript was written through contributions of all authors. All authors have given approval to the final version of the manuscript.

Notes

The authors declare no competing financial interest.

ACKNOWLEDGMENTS

The work leading to these results has received funding from the European Community's Seventh Framework Programme (FP7/2007-2013) under Grant Agreement No. NMP3-SL-2009-228631 (Project DoubleNanoMem), from the U.K. Engineering and Physical Sciences Research Council (EPSRC Grants EP/F060858/1, EP/G065144/1 and EP/G062129/1), and from the Italian national research program "Programma Operativo Nazionale Ricerca e Competitività 2007-2013,

Project PON01_01840 *MicroPERLA*." Micromeritics Instrument Corporation is thanked for provision of an ASAP 2050 high pressure sorption analyzer through the Micromeritics Grant Program. Fabio Bazzarelli is gratefully acknowledged for his assistance in some of the gas permeation experiments.

■ ABBREVIATIONS

NMR, nuclear magnetic resonance; IR, infrared

■ REFERENCES

(1) Everett, D. H. *Pure Appl. Chem.* **1972**, 577−638.
(2) Budd, P. M.; Ghanem, B. S.; Makhseed, S.; McKeown, N. B.; Msayib, K. J.; Tattershall, C. E. *Chem. Commun.* **2004**, 230−231.
(3) Carta, M.; Malpass-Evans, R.; Croad, M.; Rogan, Y.; Jansen, J. C.; Bernardo, P.; Bazzarelli, F.; McKeown, N. B. *Science* **2013**, *339*, 303−307.
(4) Du, N.; Robertson, G. P.; Song, J.; Pinnau, I.; Guiver, M. D. *Macromolecules* **2009**, *42*, 6038−6043.
(5) Weber, J.; Du, N.; Guiver, M. D. *Macromolecules* **2011**, *44*, 1763−1767.
(6) Du, N.; Park, H. B.; Robertson, G. P.; Dal-Cin, M. M.; Visser, T.; Scoles, L.; Guiver, M. D. *Nat. Mater.* **2011**, *10*, 372−375.
(7) Mason, C. R.; Maynard-Atem, L.; Al-Harbi, N. M.; Budd, P. M.; Bernardo, P.; Bazzarelli, F.; Clarizia, G.; Jansen, J. C. *Macromolecules* **2011**, *44*, 6471−6479.
(8) Patel, H. A.; Yavuz, C. T. *Chem. Commun.* **2012**, *48*, 9989−9991.
(9) Brown, H. C.; Heim, P.; Yoon, N. M. *J. Am. Chem. Soc.* **1970**, *92*, 1637−1646.
(10) Du, N.; Robertson, G. P.; Song, J.; Pinnau, I.; Thomas, S.; Guiver, M. D. *Macromolecules* **2008**, *41*, 9656−9662.
(11) Vopicka, O.; Friess, K.; Hynek, V.; Sysel, P.; Zgazar, M.; Sipek, M.; Pilnacek, K.; Lanc, M.; Jansen, J. C.; Mason, C. R.; Budd, P. M. *J. Membr. Sci.* **2013**, *434*, 148−160.
(12) Vieth, W. R.; Sladek, K. J. *J. Colloid Sci.* **1965**, *20*, 1014−1033.
(13) Crank, J. *The mathematics of diffusion*, 2nd ed.; Clarendon Press: Oxford, 1975.
(14) Zgazar, M.; Dubcova, M.; Sipek, M.; Friess, K. *Desalin. Water Treat.* **2013**, *51*, 4343−4349.
(15) Jansen, J. C.; Friess, K.; Drioli, E. *J. Membr. Sci.* **2011**, *367*, 141−151.
(16) Vishnyakov, A.; Ravikovitch, P. I.; Neimark, A. V. *Langmuir* **1999**, *15*, 8736−8742.
(17) Pinto, M. L.; Mafra, L.; Guil, J. M.; Pires, J.; Rocha, J. *Chem. Mater.* **2011**, *23*, 1387−1395.
(18) Budd, P. M.; Msayib, K. J.; Tattershall, C. E.; Ghanem, B. S.; Reynolds, K. J.; McKeown, N. B.; Fritsch, D. *J. Membr. Sci.* **2005**, *251*, 263−269.
(19) Budd, P. M.; McKeown, N. B.; Ghanem, B. S.; Msayib, K. J.; Fritsch, D.; Starannikova, L.; Belov, N.; Sanfirova, O.; Yampolskii, Y.; Shantarovich, V. *J. Membr. Sci.* **2008**, *325*, 851−860.
(20) Robeson, L. M.; Smith, Z. P.; Freeman, B. D.; Paul, D. R. *J. Membr. Sci.* **2014**, *453*, 71−83.
(21) Alentiev, A.; Yampolskii, Y. *Ind. Eng. Chem. Res.* **2013**, *52*, 8864−8874.
(22) Paul, D. R.; Kemp, D. R. *J. Polym. Sci., Polym. Symp.* **1973**, *41*, 79−93.
(23) Ghosal, K.; Chern, R. T.; Freeman, B. D.; Daly, W. H.; Negulescu, I. I. *Macromolecules* **1996**, *29*, 4360−4369.
(24) Lin, H.; Freeman, B. D. *J. Mol. Struct.* **2005**, *739*, 57−74.
(25) Struik, L. C. E. *Physical Aging in Amorphous Polymers and Other Materials*; Elsevier: Amsterdam, 1978.
(26) Huang, Y.; Paul, D. R. *Polymer* **2004**, *45*, 8377−8393.
(27) Harms, S.; Raetzke, K.; Faupel, F.; Chaukura, N.; Budd, P. M.; Egger, W.; Ravelli, L. *J. Adhes.* **2012**, *88*, 608−619.
(28) Nagai, K.; Higuchi, A.; Nakagawa, T. *J. Polym. Sci., Part B: Polym. Phys.* **1995**, *33*, 289−298.
(29) Robeson, L. M. *J. Membr. Sci.* **2008**, *320*, 390−400.
(30) Robeson, L. M. *J. Membr. Sci.* **1991**, *62*, 165−185.
(31) Emmler, T.; Heinrich, K.; Fritsch, D.; Budd, P. M.; Chaukura, N.; Ehlers, D.; Raetzke, K.; Faupel, F. *Macromolecules* **2010**, *43*, 6075−6084.
(32) Du, N.; Cin, M. M. D.; Pinnau, I.; Nicalek, A.; Robertson, G. P.; Guiver, M. D. *Macromol. Rapid Commun.* **2011**, *32*, 631−636.
(33) Li, F. Y.; Xiao, Y.; Chung, T.-S.; Kawi, S. *Macromolecules* **2012**, *45*, 1427−1437.
(34) Bushell, A. F.; Budd, P. M.; Attfield, M. P.; Jones, J. T. A.; Hasell, T.; Cooper, A. I.; Bernardo, P.; Bazzarelli, F.; Clarizia, G.; Jansen, J. C. *Angew. Chem., Int. Ed.* **2013**, *52*, 1253−1256.